

Probing non-Gaussian features in the HI distribution at the epoch of reionization

Somnath Bharadwaj¹* and Sanjay K. Pandey²†

¹ Department of Physics and Meteorology & Centre for Theoretical Studies, IIT Kharagpur, Pin: 721 302, India

² Deptt. of Mathematics, L.B.S. College, Gonda 271001, India

28 June 2018

ABSTRACT

The HI distribution at the epoch of reionization (EOR) is largely determined by the sizes and distribution of the ionized regions. In the scenario where the ionized regions have comoving sizes of the order of a few Mpc, the large scale statistical properties of the HI distribution are dominated by the Poisson noise of the discrete ionized regions, and it is highly non-Gaussian. We investigate the possibility of probing reionization by studying these non-Gaussian features using future radio interferometric observations of redshifted 21 cm HI radiation. We develop a formalism relating correlations between the visibilities measured at three different baselines and frequencies to the bispectrum of HI fluctuations. For visibilities at the same frequency, this signal is found to be of the same order as the two visibility correlation which probes the HI power spectrum. For visibilities at different frequencies, we find that the correlations decay within a frequency difference of ~ 1 MHz. This implies that it is, in principle, straightforward to extract this HI signal from various contaminants which are believed to have a continuum spectra and are expected to be correlated even at large frequency separations.

Key words: cosmology: theory - cosmology: large scale structure of universe - intergalactic medium - diffuse radiation

1 INTRODUCTION:

There has recently been a lot of interest in understanding exactly how and when the universe was reionized. There now are significant observational constraints mainly from three different kinds of observations. The observation of quasars at redshift $z \sim 6$ which show strong HI absorption (Becker et al. 2001) indicates that at least 1% of the total hydrogen mass at $z \sim 6$ is neutral (Fan et al. 2002), and the neutral mass fraction decreases rapidly at lower redshifts. This is a strong indication that the epoch of reionization ended at $z \sim 6$. Observations of the CMBR polarization, generated through Thomson scattering of CMBR photons by free electrons along the line of sight, indicates that the reionization began at a redshift $z > 14$. On the other hand, the observed anisotropies of the CMBR indicate that the total optical depth of the Thomson scattering is not extremely high, suggesting that reionization could not have started at redshift much higher than about 30 (Kogut et al. 2003; Spergel et al. 2003). A third constraint comes from determinations of the IGM temperature from observations of the Ly α forest in the z range 2 to 4 which indicates a complex reionization history with there possibly being an order unity change in the neutral hydrogen fraction at $z \leq 10$ (Theuns et al. 2002; Hui & Haiman 2003).

Mapping the HI distribution at high redshifts using radio observations of the redshifted 21 cm radiation (Madau, Meiksin & Rees 1997; Scott & Rees 1990; Kumar, Padmanabhan & Subramanian 1985) holds the possibility of probing the transition from a largely neutral to a largely ionized universe at a level of detail surpassing any other techniques. Zaldarriaga, Furlanetto & Hernquist (2003) (hereafter ZFH) have developed a statistical technique based on the angular power spectrum, on lines similar to the analysis of CMBR anisotropies, for analysing the HI signal from the epoch of reionization (EOR) in radio interferometric observations. Extracting the HI signal from various Galactic and extra Galactic contaminants (eg. Cooray &

* Email: somnathb@iitkgp.ac.in

† Email: spandey@iucaa.ernet.in

2 S. Bharadwaj and S. K. Pandey

Furlanetto 2004; DiMatteo. et al. 2004; Gnedin & Shaver 2003; Oh & Mack 2003; DiMatteo. et al. 2002; Shaver et al. 1999;) is one of the most important challenges. Most of the known contaminants are expected to have continuum spectra, and ZFH show that it should in principle be possible to extract the HI signal using the fact that, unlike the contaminants, it will be uncorrelated at two slightly different frequencies. The frequency dependence of the angular power spectrum of the HI signal and foregrounds has recently been analysed in detail by Santos, Cooray & Knox (2004).

An alternative statistical technique for analysing the HI signal is to study the correlations between the complex visibilities measured at different baselines and frequencies in radio-interferometric observations. This has been developed in the context of observing HI from $z < 6$ (Bharadwaj & Sethi 2001; Bharadwaj & Pandey 2003; Bharadwaj & Srikant 2004) and later generalized to the EOR signal in Bharadwaj & Ali 2004 (hereafter BA). The possibility of using visibility correlations to quantify the EOR signal has also been proposed by Morales & Hewitt (2003) who further discuss how the different frequency signatures of the contaminants and the HI signal can be used to distinguish between the two. Recently (Morales 2004) has addressed the issue of the power spectrum sensitivity of the EOR HI signal.

Various investigations (eg. ZFH, BA) show that the power spectrum of HI fluctuations at EOR has contributions from mainly two distinct effects, the clustering of the hydrogen which, on large scales, is assumed to follow the dark matter distribution and the fluctuations arising from the presence of discrete regions of ionized gas surrounding the sources responsible for reionizing the universe. The details of the reionization process are not very well understood (eg. Barkana & Loeb 2001), and the shape, size and distribution of these ionized regions is one of the very important issues which will be probed by 21 cm HI observations. There has recently been progress in analytically modeling the growth of the ionized regions (Furlanetto, Zaldarriaga & Hernquist 2004a) (hereafter FZH) based on the findings of simulations (Ciardi et al. 2003; Sokasian et al. 2003a; Sokasian et al. 2003b; Nusser et al. 2002; Benson et al. 2001; Gnedin 2000) which show that there will not be a large number of small HII regions around individual ionizing sources, rather there will be a few large ionized regions centered on places where the ionized sources are clustered. The size of these ionized regions are expected to be around a few Mpc (comoving) or possibly larger at EOR. In such a scenarios, on scales larger than the size of the individual ionized regions, the HI signal will be dominated by the Poisson noise arising from the discrete nature of the ionized regions (eg. ZFH, BA, FZH, Furlanetto, Zaldarriaga & Hernquist 2004b). Further, the HI signal is expected to be highly non-Gaussian .

Nearly all of the work on quantifying the EOR HI signal expected in radio interferometric observations has focused on the two point statistics namely the angular power spectrum and the correlations between pairs of visibilities. Both these quantities are actually equivalent and they basically probe the power spectrum of HI fluctuations at EOR. The power spectrum completely quantifies a Gaussian random field, but the higher order statistics would contain independent information if the HI fluctuations at EOR were not a Gaussian random field. FZH have used the pixel distribution function, a one-point statistics, to quantify non-Gaussian features in the HI distribution. He et al. (2004) have studied the non-Gaussian features that arise in the HI distribution in the log-normal model.

In this paper we address the issue of quantifying the non-Gaussian features of the HI signal expected in radio interferometric observations. In particular, we focus on the correlation between three visibilities. This is expected to be zero if the signal were a Gaussian random field, and deviations from zero are a clear signature of the non-Gaussian properties of the HI distribution. Here we derive the relation between the three visibility correlation and the bispectrum of the HI fluctuations. The bispectrum quantifies correlations between three Fourier modes, and this is non-zero only when there are phase correlations between different modes. The three visibility correlation, as we show, is comparable to the correlations between two visibilities and this leads us to speculate that this will play an important role in detecting the HI signal. Further, the higher order correlations contains independent information, and observing these would throw independent light on the topology and morphology of the HI distribution at EOR.

Finally, an outline of the paper. In Section 2. we present the formalism relating the three visibility correlation to the HI bispectrum. In Section 3. we introduce a simple model for the HI distribution at reionization and calculate its bispectrum. In Section 4. we present results for the three visibility correlation expected from HI at reionization and discuss some consequences.

It may also be noted that we use the values $(\Omega_{m0}, \Omega_{\lambda0}, \Omega_b h^2, h) = (0.3, 0.7, 0.02, 0.7)$ for the cosmological parameters throughout.

2 FORMALISM FOR THREE VISIBILITY CORRELATION

In this section we follow the notation used in BA which also contains a more detailed discussion of the formalism for calculating the HI signal. The HI radiation at frequency 1420 MHz in the rest frame of the hydrogen is redshifted to a frequency $\nu = 1420/(1+z)$ MHz for an observer at present. The expansion of the universe and the HI peculiar velocity both contribute to the redshift. Incorporating these effects, the specific intensity $I_\nu(\hat{\mathbf{n}})$ of redshifted 21 cm HI radiation at frequency ν and direction $\hat{\mathbf{n}}$ can be written as $I_\nu(\hat{\mathbf{n}}) = \bar{I}_\nu(z) \times \eta_{\text{HI}}(\hat{\mathbf{n}}, z)$ where

$$\bar{I}_\nu = 2.5 \times 10^2 \frac{\text{Jy}}{\text{sr}} \left(\frac{\Omega_b h^2}{0.02} \right) \left(\frac{0.7}{h} \right) \frac{H_0}{H(z)}. \quad (1)$$

and

$$\eta_{\text{HI}}(\hat{\mathbf{n}}, z) = \frac{\rho_{\text{HI}}}{\bar{\rho}_{\text{H}}} \left(1 - \frac{T_\gamma}{T_s} \right) \left[1 - \frac{(1+z)}{H(z)} \frac{\partial v}{\partial r} \right]. \quad (2)$$

It should be noted that the terms on the right hand side of equations (1) and (2) refer to the epoch when the HI radiation originated. Here $H(z)$ the Hubble parameter, $\bar{\rho}_{\text{H}}$ the mean cosmological density of hydrogen and r (or r_ν) the comoving distance to the HI calculated ignoring peculiar velocities, depend only on z . The quantities ρ_{HI} the HI density, T_γ the CMBR temperature, T_s the HI spin temperature and v the radial component of the HI peculiar velocity also vary with position and should be evaluated at $\mathbf{x} = r_\nu \hat{\mathbf{n}}$ *i.e.* the position where the radiation originated. It may be noted that $\eta_{\text{HI}}(\mathbf{x}, z)$, the 21cm radiation efficiency, was originally introduced by Madau, Meiksin & Rees (1997) who did not include peculiar velocities. As shown in BA, equation (2) includes an extra term which arises when the effect of the HI peculiar velocities are included. The quantity $\eta_{\text{HI}}(\hat{\mathbf{n}}, z)$ incorporate the details of the HI evolution including effects of heating, reionization and density fluctuations due to structure formation.

We next introduce $\tilde{\eta}_{\text{HI}}(\mathbf{k}, z)$, the Fourier transform of $\eta_{\text{HI}}(\mathbf{y}, z)$,

$$\eta_{\text{HI}}(\mathbf{y}, z) = \int \frac{d^3 k}{(2\pi)^3} e^{-i \mathbf{k} \cdot \mathbf{y}} \tilde{\eta}_{\text{HI}}(\mathbf{k}, z). \quad (3)$$

where \mathbf{y} refers to an arbitrary comoving position. Using this we can express $\eta_{\text{HI}}(\hat{\mathbf{n}}, z)$ as

$$\eta_{\text{HI}}(\hat{\mathbf{n}}, z) = \int \frac{d^3 k}{(2\pi)^3} e^{-i \mathbf{k} \cdot r_\nu \hat{\mathbf{n}}} \tilde{\eta}_{\text{HI}}(\mathbf{k}, z) \quad (4)$$

where it is understood that this refers to the position $\mathbf{x} = r_\nu \hat{\mathbf{n}}$.

The ensemble average of various products of $\tilde{\eta}_{\text{HI}}(\mathbf{k}_1, z)$ are used to quantify the statistical properties of the fluctuation in the HI distribution. We first consider the HI power spectrum $P_{\text{HI}}(\mathbf{k}_1, z)$ defined through

$$\langle \tilde{\eta}_{\text{HI}}(\mathbf{k}_1, z) \tilde{\eta}_{\text{HI}}(\mathbf{k}_2, z) \rangle = (2\pi)^3 \delta_D^3(\mathbf{k}_1 + \mathbf{k}_2) P_{\text{HI}}(\mathbf{k}_1, z) \quad (5)$$

where δ_D^3 is the three dimensional Dirac delta function. The power spectrum completely quantifies all properties of the HI distribution if the fluctuations are a Gaussian random field. The higher order statistics contain independent information if the fluctuations are not a Gaussian random field. Here we proceed one step beyond the power spectrum and also consider the HI bispectrum $B_{\text{HI}}(\mathbf{k}_1, \mathbf{k}_2, \mathbf{k}_3, z)$ defined through

$$\langle \tilde{\eta}_{\text{HI}}(\mathbf{k}_1, z) \tilde{\eta}_{\text{HI}}(\mathbf{k}_2, z) \tilde{\eta}_{\text{HI}}(\mathbf{k}_3, z) \rangle = (2\pi)^3 \delta_D^3(\mathbf{k}_1 + \mathbf{k}_2 + \mathbf{k}_3) B_{\text{HI}}(\mathbf{k}_1, \mathbf{k}_2, \mathbf{k}_3, z). \quad (6)$$

We next mention a few well known properties of the power spectrum and bispectrum which are relevant to the discussion. The fact that not all modes are correlated, reflected in the Dirac delta functions in eq. (5) and (6), is a consequence of the assumption that HI fluctuations are statistical homogeneous. Further, $P_{\text{HI}}(\mathbf{k})$ is isotropic *i.e.* does not depend on the direction of \mathbf{k} , if the effects of the peculiar velocity are ignored. The redshift space distortion caused by the peculiar velocities breaks the isotropy of $P_{\text{HI}}(\mathbf{k})$ which now depends on the orientation of \mathbf{k} with respect to the line of sight. Similarly, ignoring redshift space distortions, $B_{\text{HI}}(\mathbf{k}_1, \mathbf{k}_2, \mathbf{k}_3)$ depends only on the triangle formed by the wave vectors $\mathbf{k}_1, \mathbf{k}_2$ and \mathbf{k}_3 , and this is completely specified by the magnitude of the three vectors (k_1, k_2, k_3) . The bispectrum also depends on how the triangle is oriented with respect to the line of sight if redshift space distortions are included. Finally, we note that both the power-spectrum and the bispectrum are real quantities. While the power spectrum is necessarily positive, there is no such restriction on the bispectrum.

We now shift our attention to radio interferometric observations of redshifted HI using an array of low frequency radio antennas distributed on a plane. The antennas all point in the same direction \mathbf{m} which we take to be vertically up wards. The beam pattern $A(\theta)$ quantifies how the individual antenna, pointing up wards, responds to signals from different directions in the sky. This is assumed to be a Gaussian $A(\theta) = e^{-\theta^2/\theta_0^2}$ with $\theta_0 \ll 1$ *i.e.* the beam width of the antennas (in radians) is small, and the part of the sky which contributes to the signal can be well approximated by a plane. In this approximation the unit vector $\hat{\mathbf{n}}$ can be represented by $\hat{\mathbf{n}} = \mathbf{m} + \vec{\theta}$, where $\vec{\theta}$ is a two dimensional vector in the plane of the sky. Using this the angular fluctuations in the specific intensity δI_ν can be expressed as

$$\delta I_\nu(\hat{\mathbf{n}}) = \bar{I}_\nu \int \frac{d^3 k}{(2\pi)^3} e^{-i r_\nu (k_{\parallel} + \mathbf{k}_{\perp} \cdot \vec{\theta})} \tilde{\eta}_{\text{HI}}(\mathbf{k}, z) \quad (7)$$

where $k_{\parallel} = \mathbf{k} \cdot \mathbf{m}$ and \mathbf{k}_{\perp} are respectively the components of \mathbf{k} parallel and perpendicular to \mathbf{m} . The component \mathbf{k}_{\perp} lies in the plane of the sky.

The quantity measured in interferometric observations is the complex visibility $V(\mathbf{U}, \nu)$ which is recorded for every independent pair of antennas at every frequency channel in the band of observations. For any pair of antennas, $\mathbf{U} = \mathbf{d}/\lambda$ quantifies the separation \mathbf{d} in units of the wavelength λ , we refer to this dimensionless quantity \mathbf{U} as a baseline. A typical radio interferometric array simultaneously measures visibilities at a large number of baselines and frequency channels, and

$$V(\mathbf{U}, \nu) = \int d^2\theta A(\vec{\theta}) I_\nu(\vec{\theta}) e^{-i2\pi\mathbf{U}\cdot\vec{\theta}}. \quad (8)$$

The visibilities record only the angular fluctuations in $I_\nu(\theta)$ and the visibilities arising from angular fluctuations in the HI radiation are

$$V(\mathbf{U}, \nu) = \bar{I}_\nu \int \frac{d^3k}{(2\pi)^3} a(\mathbf{U} - \frac{r_\nu}{2\pi} \mathbf{k}_\perp) \tilde{\eta}_{\text{HI}}(\mathbf{k}, z) e^{-ik_\parallel r_\nu} \quad (9)$$

where $a(U)$ the Fourier transform of the antenna beam pattern $A(\theta)$, which for a Gaussian beam $A(\theta) = e^{-\theta^2/\theta_0^2}$ gives the Fourier transform also to be a Gaussian $a(\mathbf{U}) = \pi\theta_0^2 \exp[-\pi^2\theta_0^2 U^2]$ which we use in the rest of this paper.

In this paper we quantify the statistical properties of the quantity measured in radio-interferometric observations, namely the visibilities at different baselines and frequencies. Further, we study their relation to the statistical properties of the HI distribution. To this end, we introduce the notation

$$S_2(\mathbf{U}_1, \mathbf{U}_2, \Delta\nu) = \langle V(\mathbf{U}_1, \nu + \Delta\nu) V(\mathbf{U}_2, \nu) \rangle \quad (10)$$

and

$$S_3(\mathbf{U}_1, \mathbf{U}_2, \mathbf{U}_3, \Delta\nu_1, \Delta\nu_2) = \langle V(\mathbf{U}_1, \nu + \Delta\nu_1) V(\mathbf{U}_2, \nu + \Delta\nu_2) V(\mathbf{U}_3, \nu) \rangle \quad (11)$$

to denote the correlations between the visibilities at different baselines and frequencies. It should be noted that although we have shown S_2 and S_3 as explicit functions of only the frequency differences $\Delta\nu$, all these correlations also depend on the the central value ν which is not shown as an explicit argument. Further, throughout our analysis we assume that all frequency differences are much smaller than the central frequency *ie.* $\Delta\nu/\nu \ll 1$.

The correlation $S_2(\mathbf{U}_1, \mathbf{U}_2, \Delta\nu)$ between the visibilities at two baselines and frequencies has been calculated earlier (Bharadwaj & Sethi 2001; Bharadwaj & Pandey 2003; BA) who find that $S_2 \sim 0$ if $\mathbf{U}_2 \neq -\mathbf{U}_1$. This is a consequence of the statistical homogeneity of the HI fluctuations. It is sufficient to restrict the analysis to $\mathbf{U}_1 = -\mathbf{U}_2 = \mathbf{U}$ which we denote as $S_2(\mathbf{U}, \Delta\nu)$, and we have

$$S_2(\mathbf{U}, \Delta\nu) = \frac{\bar{I}_\nu^2 \theta_0^2}{2r_\nu^2} \int_0^\infty dk_\parallel P_{\text{HI}}(\mathbf{k}) \cos(k_\parallel r'_\nu \Delta\nu). \quad (12)$$

where $\mathbf{k} = k_\parallel \mathbf{m} + (2\pi/r_\nu) \mathbf{U}$ and $r'_\nu = dr_\nu/d\nu$. The vector \mathbf{k} has components k_\parallel and $(2\pi/r_\nu) \mathbf{U}$ respectively parallel and perpendicular to the line of sight. The fact that $P_{\text{HI}}(\mathbf{k})$, which includes redshift distortion, is isotropic in the directions perpendicular to the line of sight implies that S_2 is isotropic in \mathbf{U} and we can write $S_2(\mathbf{U}, \Delta\nu)$. We also note that S_2 is real for the HI signal. This follows from the fact that $P_{\text{HI}}(\mathbf{k})$ is real and it is unchanged if $k_\parallel \rightarrow -k_\parallel$.

The correlation of the visibilities at three different baselines and frequencies, S_3 is the quantity of interest in this paper. This will be related to the HI bispectrum. Here, as for the power spectrum, we assume that $\Delta\nu/\nu \ll 1$, whereby the only term in eq. (9) for the visibility $V(\mathbf{U}, \nu + \Delta\nu)$ which is affected by $\nu \rightarrow \nu + \Delta\nu$ is $e^{-ik_\parallel r_\nu + \Delta\nu}$, which can be approximated as $e^{-ik_\parallel(r_\nu + r'_\nu \Delta\nu)}$.

We then have

$$S_3(\mathbf{U}_1, \mathbf{U}_2, \mathbf{U}_3, \Delta\nu_1, \Delta\nu_2) = \frac{\bar{I}_\nu^3}{(2\pi)^6} \int d^3k_1 d^3k_2 d^3k_3 a(\mathbf{U}_1 - \frac{r_\nu}{2\pi} \mathbf{k}_{1\perp}) a(\mathbf{U}_2 - \frac{r_\nu}{2\pi} \mathbf{k}_{2\perp}) \times \\ a(\mathbf{U}_3 - \frac{r_\nu}{2\pi} \mathbf{k}_{3\perp}) e^{-i(k_{1\parallel} + k_{2\parallel} + k_{3\parallel})r_\nu} e^{-i(k_{1\parallel} \Delta\nu_1 + k_{2\parallel} \Delta\nu_2)r'_\nu} \delta_D^3(\mathbf{k}_1 + \mathbf{k}_2 + \mathbf{k}_3) B_{\text{HI}}(\mathbf{k}_1, \mathbf{k}_2, \mathbf{k}_3) \quad (13)$$

It is convenient to write the d^3k integrals as $dk_\parallel d^2k_\perp$ and integrate over $dk_{3\parallel}$, whereby the term $e^{-i(k_{1\parallel} + k_{2\parallel} + k_{3\parallel})r_\nu}$ drops out because of the Dirac delta function. Also, we introduce a new variable $\mathbf{y} = \mathbf{k} - (2\pi/r_\nu) \mathbf{U}$ and use the explicit form for the function $a(\mathbf{U})$, whereby we have

$$S_3(\mathbf{U}_1, \mathbf{U}_2, \mathbf{U}_3, \Delta\nu_1, \Delta\nu_2) = \frac{\bar{I}_\nu^3}{(2\pi)^6} \int dk_{1\parallel} dk_{2\parallel} e^{-i(k_{1\parallel} \Delta\nu_1 + k_{2\parallel} \Delta\nu_2)r'_\nu} \int d^2y_1 d^2y_2 d^2y_3 \times \\ \delta_D^2[(2\pi/r_\nu)(\mathbf{U}_1 + \mathbf{U}_2 + \mathbf{U}_3) + \mathbf{y}_1 + \mathbf{y}_2 + \mathbf{y}_3] (\pi\theta_0^2)^3 \exp[-(r_\nu\theta_0/2)^2(y_1^2 + y_2^2 + y_3^2)] B_{\text{HI}} \quad (14)$$

where the arguments of the bispectrum change as we carry out the integrals, but we do not show them explicitly.

Carrying out the d^2y_3 integral we have

$$S_3(\mathbf{U}_1, \mathbf{U}_2, \mathbf{U}_3, \Delta\nu_1, \Delta\nu_2) = \frac{\bar{I}_\nu^3}{(2\pi)^6} \int dk_{1\parallel} dk_{2\parallel} e^{-i(k_{1\parallel} \Delta\nu_1 + k_{2\parallel} \Delta\nu_2)r'_\nu} \int d^2y_1 d^2y_2 \times \\ \exp[-(r_\nu\theta_0/2)^2(y_1^2 + y_2^2)] \exp[-(r_\nu\theta_0/2)^2\{\mathbf{y}_1 + \mathbf{y}_2 + (2\pi/r_\nu)(\mathbf{U}_1 + \mathbf{U}_2 + \mathbf{U}_3)\}^2] B_{\text{HI}} \quad (15)$$

The point to note is the two Gaussian functions $\exp[-(r_\nu\theta_0/2)^2(y_1^2 + y_2^2)]$ and $\exp[-(r_\nu\theta_0/2)^2\{\mathbf{y}_1 + \mathbf{y}_2 + (2\pi/r_\nu)(\mathbf{U}_1 + \mathbf{U}_2 + \mathbf{U}_3)\}^2]$ are peaked around different values of \mathbf{y}_1 and \mathbf{y}_2 . While the former is peaked around $\mathbf{y}_1 = \mathbf{y}_2 = 0$, the latter is peaked

around $\mathbf{y}_1 + \mathbf{y}_2 = (-2\pi/r_\nu)(\mathbf{U}_1 + \mathbf{U}_2 + \mathbf{U}_3)$. The peaks of the two functions have very little overlap if $|\mathbf{U}_1 + \mathbf{U}_2 + \mathbf{U}_3| > 0$, and the visibility correlations are exponentially suppressed if the vector sum of the baselines differs from zero. There are substantial correlations only for the sets of baselines for which $|\mathbf{U}_1 + \mathbf{U}_2 + \mathbf{U}_3| \leq (\pi\theta_0)^{-1}$. In the rest of our analysis we only consider combinations of baselines for which $\mathbf{U}_1 + \mathbf{U}_2 + \mathbf{U}_3 = 0$, and the product of the two Gaussian functions becomes $\exp[-2(r_\nu\theta_0/2)^2(y_1^2 + y_2^2 + \mathbf{y}_1 \cdot \mathbf{y}_2)]$. This can be further simplified if the baselines we are dealing with are much larger than $1/(\pi\theta_0)$. We can then approximate this function by a product of two Dirac delta functions $\approx (16\pi/3)(r_\nu\theta_0)^{-4}\delta_D^2(\mathbf{y}_1 + \mathbf{y}_2/2)\delta_D^2(\mathbf{y}_2)$. Using this in eq. (15) we have

$$S_3(\mathbf{U}_1, \mathbf{U}_2, \mathbf{U}_3, \Delta\nu_1, \Delta\nu_2) = \frac{\bar{I}_\nu^3 \theta_0^2}{12\pi r_\nu^4} \int dk_{1\parallel} dk_{2\parallel} e^{-i(k_{1\parallel}\Delta\nu_1 + k_{2\parallel}\Delta\nu_2)r'_\nu} B_{\text{HI}}(\mathbf{k}_1, \mathbf{k}_2, \mathbf{k}_3) \quad (16)$$

where $\mathbf{k}_1 = k_{1\parallel}\mathbf{m} + (2\pi/r_\nu)\mathbf{U}_1$, $\mathbf{k}_2 = k_{2\parallel}\mathbf{m} + (2\pi/r_\nu)\mathbf{U}_2$ and $\mathbf{k}_3 = -(k_{1\parallel} + k_{2\parallel})\mathbf{m} + (2\pi/r_\nu)\mathbf{U}_3$. Further, it can be verified that S_3 is real, and

$$S_3(U_1, U_2, U_3, \Delta\nu_1, \Delta\nu_2) = \frac{\bar{I}_\nu^3 \theta_0^2}{12\pi r_\nu^4} \int dk_{1\parallel} dk_{2\parallel} \cos[(k_{1\parallel}\Delta\nu_1 + k_{2\parallel}\Delta\nu_2)r'_\nu] B_{\text{HI}}(\mathbf{k}_1, \mathbf{k}_2, \mathbf{k}_3) \quad (17)$$

where we have also incorporated the fact that S_3 depends only the triangle formed by $\mathbf{U}_1, \mathbf{U}_2$ and \mathbf{U}_3 which is completely specified by just the magnitudes (U_1, U_2, U_3) .

We use eqs. (12) and (17) to calculate the visibility correlations expected during the epoch of reionization.

3 A MODEL FOR THE HI DISTRIBUTION

The reionization of the HI in the universe started, possibly at a redshift $z \sim 30$, when the first luminous objects were formed. The radiation from these luminous objects and from the subsequently formed luminous objects ionized the low density HI in the universe. The reionization commences in small spherical regions (Stromgren sphere) surrounding the luminous objects. These spheres are filled with ionized HII gas, the rest of the universe being filled with HI. Gradually these ionized regions grow until they finally overlap, filling up the whole of space, and all the low density gas in the universe is ionized. The HI distribution during reionization is largely determined by the ionized regions. This is expected to be highly non-Gaussian carrying signatures of the size, shape and distribution of the discrete ionized regions. Here we adopt a simple model for the ionized regions. Though simple, this model suffices to illustrate the non-Gaussian nature of the HI distribution and allows us to calculate some of the salient observable consequences.

We assume that the HI gas is heated well before it is reionized, and that the spin temperature is coupled to the gas temperature with $T_s \gg T_\gamma$ so that $(1 - T_\gamma/T_s) \rightarrow 1$. It then follows that $\eta_{\text{HI}} > 0$ (eq. 2) *ie.* the HI will be seen in emission. At any epoch a fraction of the volume f_V is completely ionized, the ionized gas being in non-overlapping spheres of comoving radius R , the centers of the spheres being randomly distributed. This model is similar to that used by ZFH in the context of HI emission, and Gruzinov & Hu (1998) and Knox et al. (1998) in the context of the effect of patchy reionization on the CMBR. One would expect the centers of the ionized spheres to be clustered, given the fact that we identify them with the locations of the first luminous objects which are believed to have formed at the peaks of the density fluctuations. This effect, included in BA, has not been taken into account here.

Following ZFH, we assume that the mean neutral fraction \bar{x}_{HI} at any epoch is given by

$$\bar{x}_{\text{HI}}(z) = \frac{1}{1 + \exp((z - z_0)/\Delta z)} \quad (18)$$

with $z_0 = 10$ and $\Delta z = 0.5$ so that 50% of the hydrogen is neutral at a redshift $z = 10$. The mean comoving number density of ionized spheres \bar{n}_{HI} is related to the quantities defined earlier as $f_V = 1 - \bar{x}_{\text{HI}} = (4\pi R^3/3)\bar{n}_{\text{HI}}$. We have kept R as a free parameter and have used this to determine \bar{n}_{HI} .

We assume that the total hydrogen density traces the dark matter and hence it is $\bar{\rho}_{\text{H}}(1+\delta)$ where δ refers to the fluctuations in the dark matter distribution. Then, in our model, the HI density is $\rho_{\text{HI}}(\mathbf{x}, z) = \bar{\rho}_{\text{H}}(1+\delta) \left[1 - \sum_a \theta(|\mathbf{x} - \mathbf{x}_a|/R) \right]$, where a refers to the different ionized spheres with centers at \mathbf{x}_a , and $\theta(y)$ is the Heaviside step function defined such that $\theta(y) = 1$ for $0 \leq y \leq 1$ and zero otherwise. We then have

$$\eta_{\text{HI}}(\mathbf{x}, z) = \left[1 + \delta - \frac{1+z}{H(z)} \frac{\partial v}{\partial r} \right] \left[1 - \sum_a \theta\left(\frac{|\mathbf{x} - \mathbf{x}_a|}{R}\right) \right]. \quad (19)$$

where v refers to the peculiar velocity caused by δ . The point to note is that $\eta_{\text{HI}}(\mathbf{x}, z)$ has contributions from two distinct effects namely the fluctuations arising from the gravitational clustering of the hydrogen which follows the dark matter distribution and the discrete ionized regions. Earlier studies (ZFH) have shown that the contribution from the discrete ionized regions dominates the HI power spectrum on length-scales larger than the size of the individual ionized bubbles at redshifts $z \sim 10$ when $f_V \sim 0.5$ and the HI signal is expected to be maximum. In the standard scenario, the initial dark matter fluctuation

δ is assumed to be a Gaussian random field for which the bispectrum is zero. Non-Gaussian features of order $\sim \delta^2$ arise from non-linear effects as the density fluctuation grow, but these effects are expected to be very small on the length scales of our interest at redshifts $z \geq 10$. The bispectrum B_{HI} too will be dominated by the non-Gaussian features arising from the discrete ionized regions. Further, we expect the gravitational clustering of the hydrogen to make a smaller contribution to the bispectrum than it does to the power spectrum. The aim here being to investigate the non-Gaussian effects through a study of the bispectrum, it is justified to focus on just the contribution arising from the individual ionized regions, ignoring the effects of gravitation clustering. Under this assumption

$$\eta_{\text{HI}}(\mathbf{x}, z) = \left[1 - \sum_a \theta\left(\frac{|\mathbf{x} - \mathbf{x}_a|}{R}\right) \right]. \quad (20)$$

and its Fourier transform for $k > 0$ is

$$\tilde{\eta}_{\text{HI}}(\mathbf{k}, z) = \frac{-f_V W(kR)}{\bar{n}_{\text{HI}}} \sum_a e^{i\mathbf{k} \cdot \mathbf{x}_a} \quad (21)$$

where $W(y) = (3/y^3)[\sin(y) - y \cos(y)]$ is the spherical top hat window function. Using these we have

$$P_{\text{HI}}(\mathbf{k}) = \frac{f_V^2 W^2(kR)}{\bar{n}_{\text{HI}}} \quad (22)$$

and

$$B_{\text{HI}}(\mathbf{k}_1, \mathbf{k}_2, \mathbf{k}_3) = -\frac{f_V^3 W(k_1 R) W(k_2 R) W(k_3 R)}{\bar{n}_{\text{HI}}^2} \quad (23)$$

respectively for the power spectrum and the bispectrum. We use these to calculate the visibility correlations expected in this model.

Our model has a limitation that it cannot be used when a large fraction of the volume is ionized as the ionized spheres start to overlap and the HI density becomes negative in the overlapping regions. Calculating the fraction of the total volume where the HI density is negative, we find this to be $f_V^2/2$. We use this to assess the range of validity of our model. We restrict the model to $z > 10$ where $f_V < 0.5$, and the HI density is negative in less than 12.5% of the total volume.

4 RESULTS AND DISCUSSION

In this section we present results for the visibility correlations expected from HI during the epoch of reionization. Our aim being to illustrate the non-Gaussian nature of the expected signal and its dependence on the ionized regions, we show results centered on only at a single frequency namely 125 MHz. This corresponds to a redshift $z = 10.4$ when the mean neutral fraction is $\bar{x}_{\text{HI}} = 0.67$ (*i.e.* $f_V = 0.33$). We choose this particular frequency as \bar{x}_{HI} is quite close to 0.5 where the HI signal is expected to be maximum, simultaneously ensuring that the volume fraction where the HI density predicted by our model becomes negative is small ($\sim 5\%$). Further, the HI signal is expected to be dominated by discrete ionized regions and hence we anticipate significant non-Gaussian features.

We have used eqs. (12) and (17) to calculate the expected correlations between two and three visibilities respectively. For this it is necessary to specify a value for θ_0 , the beam size of the individual antennas in the array. Further, it may be noted that $\theta_0 \approx 0.6 \times \theta_{\text{FWHM}}$. The value of θ_0 will depend on the physical dimensions of the antennas and the wavelength of observation. For the GMRT $\theta_0 = 1^\circ$ at 325 MHz. We scale this using $\theta_0 \propto \lambda$ to obtain $\theta_0 = 2.6^\circ$ at 125 MHz which we use here. The HI signal predicted here is for observations using the GMRT, and they can be directly compared to those in BA. Both S_2 and S_3 scale as θ_0^2 , and it is straightforward to scale the results presented here to make visibility correlation predictions for other radio telescopes.

The comoving radius of the ionized spheres R is a free parameter in our model. Investigations on the growth of the ionized spheres (FZH) show that these will be at least a few Mpc in radius (possibly larger) at the redshift of interest. We have considered three possible values $R = (1, 3, 5) h^{-1} \text{ Mpc}$ for which the respective values of \bar{n}_{HI} are $(78, 2.9, 0.63) \times 10^{-3} h^3 \text{ Mpc}^{-3}$.

For ease of graphical presentation, we have restricted our analysis of S_3 to equilateral triangles for which the size of the baseline U completely specifies the triangle, and we have $S_3(U, \Delta\nu)$. Further, we first consider the correlations at the same frequency *i.e.* $\Delta\nu = 0$ Figures (1) and (2) show the results $[S_2(U)]^{1/2}$ and $[-S_3(U)]^{1/3}$ respectively.

We find that at small U , $[S_2(U)]^{1/2}$ is more or less constant with a value of the order of $\sim 0.2 \text{ mJy}$ for $R = 3 h^{-1} \text{ Mpc}$. The signal is proportional to $R^{3/2}$ and its magnitude increases as the ionized spheres become larger. Each baseline U can be associated with a comoving length-scale $r_\nu/(2\pi U)$ at the comoving distance where the HI radiation originated. The signal from the ionized spheres is constant across the baselines for which $r_\nu/(2\pi U)$ is larger than the size of the spheres, and the signal falls at baselines for which $U > r_\nu/(2\pi R)$. Each baseline resolves out features larger than $r_\nu/(2\pi U)$, and the

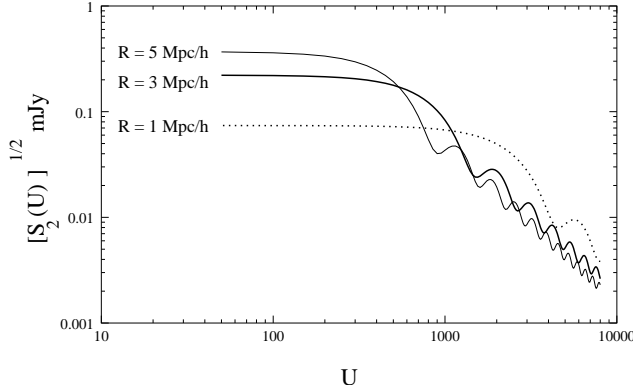


Figure 1. This shows the visibility correlation $S_2(U, \Delta\nu)^{1/2}$ as a function of U for $\Delta\nu = 0$, for different values of R , the comoving radius of the ionized spheres. These predictions are for observations centered at 125 MHz.

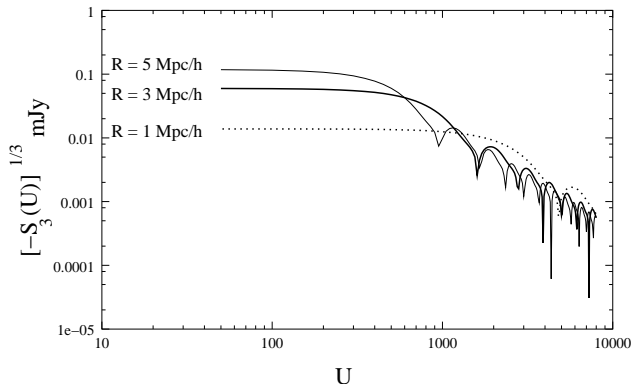


Figure 2. This shows the visibility correlation $[-S_3(U, \Delta\nu)]^{1/3}$ as a function of U for $\Delta\nu = 0$, for different values of R , the comoving radius of the ionized spheres. These predictions are for observations centered at 125 MHz.

presence of discrete ionized regions make very little contribution to the signal at the large baselines. Comparing the results for $[S_2(U)]^{1/2}$ presented here with those presented in BA which also includes the effects of gravitational clustering, we note that the gravitational clustering signal is also of the order ~ 0.1 mJy at small U . The gravitational clustering signal also falls with increasing U , and the combined signal would depend critically on the size of the bubbles. For example, the signal from discrete ionized sources would dominate over the gravitational clustering signal at baselines $U > 500$ if the ionized spheres had comoving radius $R = 5 h^{-1}$ Mpc, whereas the gravitational clustering signal would possibly dominate throughout for $R = 1 h^{-1}$ Mpc.

Turning our attention next to S_3 (Figure 2), the first point to note is that this is negative. The shape of S_3 as a function of U is very similar to that of S_2 , and its magnitude is around $[-S_3(U)]^{1/3} \sim 0.06$ mJy at $R = 3 h^{-1}$ Mpc, which is around three times smaller than $[S_2(U)]^{1/2}$. At small U , $[-S_3(U)]^{1/3}$ is more or less constant. Although our results are restricted to equilateral triangles, we expect the correlations to be nearly constant for triangles of all shapes provided all the baselines satisfy $U < r_\nu/(2\pi R)$. The signal is proportional to R^2 and its magnitude increases a little faster than that of $[S_2(U)]^{1/2}$ as R is increased. We expect the dark matter density fluctuations at $z > 10$ to be well in the linear regime on comoving length-scales $\sim 10 h^{-1}$ Mpc or larger, and the contribution to S_3 from non-linear gravitational clustering is expected to be very small on these scales. It may be noted that the contribution to S_3 from linear gravitational clustering is exactly zero in the standard scenario where the initial density fluctuations are a Gaussian random field. Further, the comoving length-scale $10 h^{-1}$ Mpc corresponds to the baseline $U \sim 100$ and we expect the contribution from individual ionized spheres considered here to be the dominant signal at these baselines.

We next consider the correlations between the visibilities at different frequencies. Again, for ease of graphical presentation we have restricted our analysis of $S_3(U, \Delta\nu_1, \Delta\nu_2)$ to equilateral triangles with the added restriction that $\Delta\nu_1 = \Delta\nu_2 = \Delta\nu$, so we have $S_3(U, \Delta\nu)$. We have shown results only for $R = 3 h^{-1}$ Mpc, but a similar behaviour is expected for other values also. We find that both $S_2(U, \Delta\nu)$ and $S_3(U, \Delta\nu)$ fall rapidly, in nearly the same fashion independent of U , and are very close to zero by $\Delta\nu \approx 0.5$ MHz.

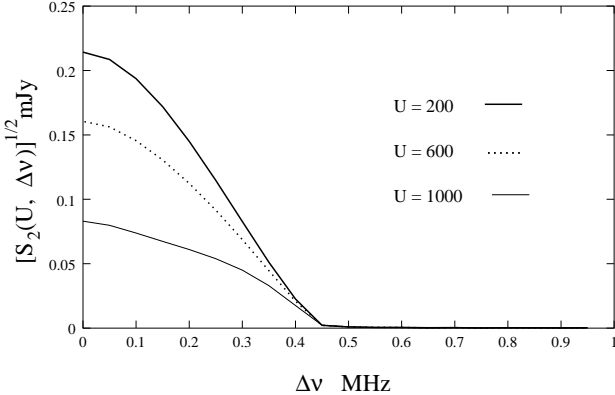


Figure 3. This shows the visibility correlation $S_2(U, \Delta\nu)^{1/2}$ as a function of $\Delta\nu$ for the three different values of U shown in the figure. The comoving radius of the ionized spheres is assumed to be $R = 3 h^{-1}$ Mpc and the predictions are for observations centered at 125 MHz.

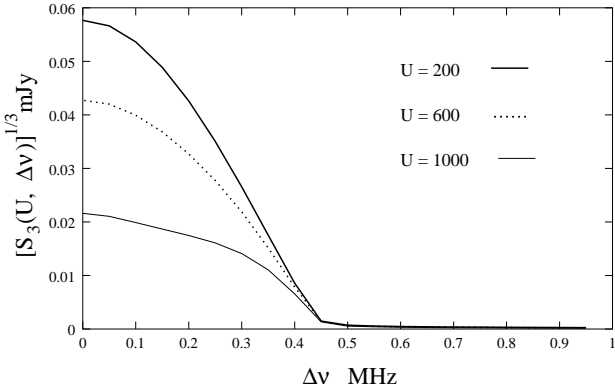


Figure 4. This shows the visibility correlation $[-S_3(U, \Delta\nu)]^{1/3}$ as a function of $\Delta\nu$ for the three different values of U shown in the figure. The comoving radius of the ionized spheres is assumed to be $R = 3 h^{-1}$ Mpc and the predictions are for observations centered at 125 MHz.

One of the main challenges in observing cosmological HI is to extract it from various contaminants which are expected to swamp this signal. The contaminants include Galactic synchrotron emission, free-free emission from ionizing halos (Oh & Mack 2003), faint radio loud quasars (DiMatteo. et al. 2002) and synchrotron emission from low redshift galaxy clusters (DiMatteo. et al. 2004). Fortunately, all of these foregrounds have smooth continuum spectra and we expect their contribution to the visibilities to be correlated over large $\Delta\nu$, whereas the HI contribution is uncorrelated beyond 1 MHz or less. It is, in principle, straightforward to fit the visibility correlations S_2 and S_3 at large $\Delta\nu$ and remove any slowly varying component thereby separating the contaminants from the HI signal. We also use this opportunity to note that this is a major advantage of using visibility correlations as compared to the angular power spectrum which exhibits substantial correlations even at two frequencies separated by ~ 10 MHz (Santos, Cooray & Knox 2004).

An important fact which emerges from our analysis is that the HI signal in the correlation between three visibilities is of the same order as the correlation between two visibilities, the former being around three times smaller. This is a generic feature of the EOR HI signal, valid if the ionized regions are bubbles of the size $R = 1 h^{-1}$ Mpc or larger. This signal arises from the Poisson noise of the discrete ionized regions, and it is enhanced if the size of the bubbles is increased. The fact that there is a substantial S_3 tells us that there are large phase correlations between the visibilities. This is a consequence of the fact that there are only a few coherent features (the ionized regions) which dominate the whole HI signal.

Investigations on the growth of ionized regions (FZH) show that there will be a spread in the sizes of the ionized regions at any given epoch. This will smoothen some of the sharp features seen in Figures (1) and (2). The ringing seen in the these figures is an artifact of there being only a single value of R and we do not expect this feature to be there if we have a spread in R . Further, the gravitational clustering signal not shown here may also dominate at large U . Despite all these limitations, we can still expect substantial correlations between three visibilities in a more realistic analysis, this being a robust signature of the fact that reionization occurs through a few, large ($R \sim$ a few Mpc) bubbles of ionized gas and the HI signal is dominated by Poisson noise.

We next briefly discuss the noise levels and the integration times required to observe the HI signal, particularly addressing

the question whether S_3 can be detected with integration times comparable to those needed for S_2 . We consider an array of N antennas, the observations lasting a time duration t , with frequency channels of width $\delta\nu$ spanning a total bandwidth B . It should be noted that the effect of a finite channel width $\delta\nu$ has not been included in our calculation which assumes infinite frequency resolution. This effect can be easily included by convolving our results for the visibility correlation with the frequency response function of a single channel. Preferably, $\delta\nu$ should be much smaller than the frequency separation at which the visibility correlation become uncorrelated. We use S to denote the frequency separation within which the visibilities are correlated, and beyond which they become uncorrelated.

We use N_2 and N_3 to denote the rms. noise in S_2 and S_3 respectively. It is well known that $N_2 = \left(\frac{2k_B T_{SYS}}{A_{ef}}\right)^2 \frac{1}{\delta\nu t}$ (Thompson, Moran & Swenson 1986), and we have $N_3 \sim \left(\frac{2k_B T_{SYS}}{A_{ef}}\right)^3 \frac{1}{(\delta\nu t)^{3/2}}$ assuming that we have Gaussian random noise, where T_{SYS} is the system temperature and A_{ef} is the effective area of a single antenna. The noise contributions will be reduced by a factor $1/\sqrt{N_o}$ if we combine N_o independent samples of the visibility correlation. A possible observational strategy for a preliminary detection of the HI signal would be to combine the visibility correlations at all baselines and frequency separations where there is a reasonable amount of signal. This gives $N_o = [N(N-1)/2](B/\delta\nu)(S/\delta\nu)$ for the two visibility correlation and $N_o = [N(N-1)(N-2)/6](B/\delta\nu)(S/\delta\nu)^2$ for the three visibility correlations. It should be noted that we have used the fact that the S_3 is non-zero only for the baselines between triplets of antennas. Combining all of this we have $[N_2]^{1/2} \sim \left(\frac{2k_B T_{SYS}}{A_{ef}}\right) \left[\frac{2}{N(N-1)BS}\right]^{1/4} \frac{1}{t^{1/2}}$ and $[N_3]^{1/3} \sim \left(\frac{2k_B T_{SYS}}{A_{ef}}\right) \left[\frac{6}{N(N-1)(N-2)BS^2}\right]^{1/6} \frac{1}{t^{1/2}}$. The ratio $[N_3]^{1/3}/[N_2]^{1/2} \sim [N(N-1)B/(N-2)^2 S]^{1/12}$ has a very weak dependence on N , B and S for a reasonable choice of values, and is of order unity. We thus see that, for a given integration time, we will achieve comparable noise levels in both the two and three visibility correlations. Estimates of the integration time to detect S_2 (or equivalently the angular power spectrum) (BA, ZFH) indicate this to be around a few hundred hours. We find that it should be possible to also detect S_3 in a comparable integration time.

ACKNOWLEDGMENTS

SB would like to thank Sk. Saiyad Ali and Jayaram Chengalur for useful discussions. SB would also like to acknowledge BRNS, DAE, Govt. of India, for financial support through sanction No. 2002/37/25/BRNS. SKP would like to acknowledge the Associateship Program, IUCAA for support.

REFERENCES

- Barkana R. & Loeb A., 2001, Phys. Rep., 349, 125
- Becker, R.H., et al., 2001, AJ, 122, 2850
- Benson, A. J., Nusser, A., Sugiyama, N., & Lacey, C. G. 2001, MNRAS, 320, 153
- Bharadwaj, S. & Sethi, S. K. 2001, JApA, 22, 293
- Bharadwaj, S. & Pandey, S. K. 2003, JApA, 24, 23
- Bharadwaj, S. & Srikant p,s. 2004, JApA, in press
- Bharadwaj S. & Ali S. S. 2004, MNRAS, in Press, astro-ph/0406676
- Ciardi, B. , Stoehr, & White, S.D.M. 2003, MNRAS, 343, 1101
- Cooray, A. & Furlanetto, S. 2004, Ap.J, 606, L5-L8
- DiMatteo, T., Ciardi, B., Miniati, F. 2004, MNRAS, submitted, astro-ph/0402332
- DiMatteo, T., Perna, R., Abel, T., Rees, M.J. 2002, Ap.J, 564, 576
- Fan, X., et al. 2002, AJ, 123, 1247
- He, P., Liu, J., Feng, L.L., Bi, H.G. & Fang, L.Z., 2004, Ap.J, 614, 6
- Furlanetto, S. R., Zaldarriaga, M. & Hcernquist L. 2004a, astro-ph/0403697
- Furlanetto, S. R., Zaldarriaga, M. & Hcernquist L. 2004b, astro-ph/0404112
- Gnedin, N. Y. 200, Ap.J, 535, 530
- Gnedin, N. Y. & Shaver, P. A. 2004, 608, 611
- Gruzinov, A. & Hu, W. 1998, Ap.J, 508, 435
- Hui, L., & Haiman, Z., 2003, ApJ, 596, 9
- Kogut et al, 2003, ApJS, 148, 161
- Kumar A., Padmanabhan T. and Subramanian K., 1995, MNRAS, 272, 544
- Knox L., Scoccimarro R. & Dodelson S. 1998, Physical Review Letters, 81, 2004
- Madau P., Meiksin A. & Rees, M. J., 1997, Ap.J, 475, 429
- Morales, M. F. 2004, preprint, astro-ph/0406662

Morales, M. F. and Hewitt, J., 2003, ApJ, Submitted (astro-ph/0312437)
Nusser, A., Benson, A. J., Sugiyama, N., & Lacey, C. 2002, ApJL, 580, L93
Oh,S.P.,& Mack,K.J.,2003,MNRAS,346,871
Santos, M.G., Cooray, A. & Knox, L. 2004, preprint, astro-ph/0408515
Scott D. & Rees, M. J., 1990, MNRAS,247,510
Shaver, P. A., Windhorst, R. A., Madau, P.& de Bruyn, A. G.,1999, A & A, 345, 380
Sokasian, A. Abel, T. Hernquist, L. & Springel, V. 2003a, MNRAS, 344, 607
Sokasian, A., Yoshida, N., Abel, T., Hernquist, L. & Springel, V.S. 2003b, 350, 47
Spergel, D. N.,et al. 2003,ApJS,148,175
Theuns, T. et al., 2002, ApJ,567,L103
Thompson, A.R., Moran, J.M. and Swenson, G.W., Jr. 1986, Interferometry and Synthesis in Radio Astronomy, John Wiley and Sons, New York, pp 162-165
Zaldarriaga M., Furlanetto, S. R. & Hernquits L., 2003, Ap.J, 608, 622